LIGHT-INDUCED INTERFACIAL POTENTIALS IN PHOTORECEPTOR MEMBRANES

DAVID S. CAFISO AND WAYNE L. HUBBELL, *The Department of Chemistry, University of California, Berkeley, California 94720 U.S.A.*

ABSTRACT A rapid change in an interfacial electric potential of isolated bovine rod outer-segment disk membranes occurs upon illumination. This potential change, which has been detected by the use of spin-labeled hydrophobic ions, apparently occurs within a low dielectric boundary region of the membrane near the external (cytoplasmic) surface and is positive with respect to the aqueous exterior of the disk. The magnitude of the potential change is pH- and temperature-dependent and appears with a first-order half-time of ~7 ms at 21°C. A simple model in which one positive charge per bleached rhodopsin is translocated from the cytoplasmic aqueous space into the membrane low dielectric boundary region readily accounts for all experimental observations. The great similarity of the boundary potential change to the R_2 phase of the early receptor potential suggests that the two have the same molecular origin.

INTRODUCTION

Hydrophobic ions, such as tetraphenylboron and triphenylmethyl phosphonium, appear to bind to a region of bilayer membranes which is located near, but not at the membrane-solution interface (Ketterer et al., 1971; Andersen and Fuchs, 1975; Andersen et al., 1978). This region will be referred to as the "boundary region." The absorption of charge in this low dielectric region results in the establishment of an electrostatic potential within the membrane interior termed the "boundary potential" (Andersen et al., 1978; McLaughlin, 1977). Unlike surface potentials which arise from charge absorbed at the membrane-solution interface, boundary potentials arising from charge absorbed in the boundary layer are not abolished in high ionic strength media. Boundary potentials have recently been indirectly observed in model membranes (Andersen et al., 1978), but their significance, if any, in biological membranes is not yet known. It has been suggested that changes in the boundary potential may be associated with the gating of ion channels in excitable membranes (Hong, 1977; Lundström, 1977).

We have recently shown that spin-labeled hydrophobic phosphonium ions (Cafiso and Hubbell, 1978*a*) can be used to estimate transmembrane potentials in phospholipid vesicles. In the present paper, we show that the same labels may, in addition, be used to detect rapid changes in boundary potentials in rod outer-segment (ROS)[1] disk membranes. In these

Dr. Hubbell is a Dreyfus Foundation Scholar. Dr. Cafiso is a fellow of the Jane Coffin Childs Memorial Fund for Medical Research.

[1] *Abbreviations used in this paper:* CCCP, carbonylcyanide *m*-chlorophenylhydrazone; ERP, early receptor potential. ESR, electron spin resonance; MI, metarhodopsin I; MII, metarhodopsin II; MES, morpholinoethanesulfonic acid; MOPS, morpholinopropanesulfonic acid; ROS, rod outer segment; TEMPO, 2,2,6,6-tetramethylpiperidine-1-oxyl.

membranes, we have measured a change in boundary potential which is initiated by the absorption of a photon by rhodopsin (Cafiso and Hubbell, 1979).

EXPERIMENTAL

Spin Labels

In the present study, we have made use of the following set of spin labels:

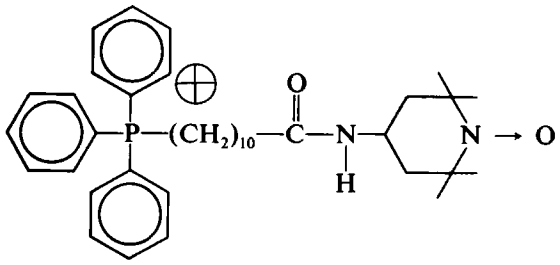

I

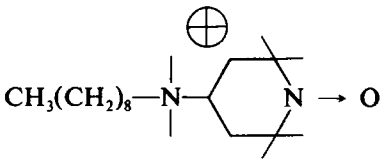

II

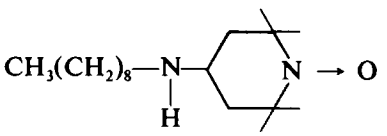

III

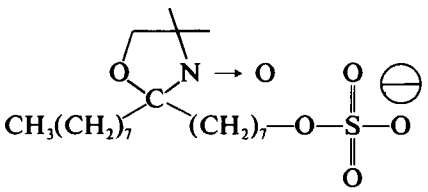

IV

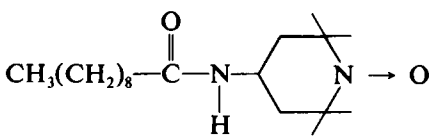

V

The phosphonium spin label I was synthesized as previously described (Cafiso and Hubbell, 1978*a*) except that the phosphobetaine was condensed with 1-amino-2,2,6,6-tetramethylpiperidine-1-oxyl rather than 1-hydroxy-2,2,6,6-tetramethylpiperidine-1-oxyl. The quaternary ammonium spin label II and secondary amine spin label III were prepared as previously described (Castle and Hubbell, 1976; Cafiso and Hubbell, 1978*b*). The sulfate ester spin label IV was a generous gift of J. David Castle (Yale University, New Haven, Conn.). The amide spin label V was synthesized according to Waggoner et al. (1967).

ROS Disk Membranes

ROS disk membranes were isolated from dark-adapted bovine retinas (American Stores Packing Co., Lincoln, Neb.) by a modification of a method given previously (Sale et al., 1977). Sucrose solutions all

contained 0.067 M potassium phosphate buffer, pH = 7.0, and all operations were carried out at 4°C under dim red light or in total darkness. 50 partially thawed retinas were ground in a mortar until smooth, 45% wt/vol sucrose was then added to a volume of ~80 ml and the suspension was centrifuged at 9,000 *g* for 20 min. The supernate was collected and diluted with ~90 ml of buffer and centrifuged at 39,000 *g* for 20 min to pellet the ROS. The crude membranes were then homogenized with 32% wt/vol sucrose and the total volume was adjusted to 18.5 ml with this sucrose solution. This suspension was layered onto a sucrose step gradient of 36% wt/vol (10 ml), 34% wt/vol (5 ml), and 32% wt/vol (5 ml) in a 38.5-ml tube; the system was brought to equilibrium by centrifugation for 1 h at 130,000 *g*. The ROS disk membranes which banded at the 34/32 and 34/36% wt/vol interfaces were collected, diluted with an equal volume of buffer, and centrifuged at 39,000 *g* for 20 min. The pellet was washed three times with 10 mM Naphosphate, pH = 6.8, then washed and suspended in the desired buffer. Typical yields were 0.6–0.7 mg of rhodopsin/retina with an absorbance ratio A_{278}/A_{498} of ≤ 2.5. The ROS membranes were obtained in the form of closed spherical vesicles ~0.5 μm in diameter (Norisuye et al., 1976).

ROS membranes from fresh retinas obtained locally were prepared in a manner similar to that described for frozen retinas except that the fresh retinas were not ground or homogenized but were instead shaken in 45% wt/vol sucrose. The ROS from the first floatation were then homogenized in 18.5 ml of 26.4% wt/vol sucrose (~25 retinas worth of crude ROS) and layered onto 20 ml of 32.5% sucrose and processed as before to purify the crude ROS. ROS prepared in this way had ratios A_{278}/A_{498} comparable to the dark-adapted frozen retinas but with yields that were lower (typically 0.3–0.5 mg of rhodopsin per retina).

For spin label experiments, ROS membranes were typically used at concentrations containing 4 mg/ml of rhodopsin with spin label concentrations of 35 μM, unless otherwise stated. For experiments designed to estimate the relative binding constants of spin label I to the internal and external sides of the membrane, ROS from fresh retinas were isolated as above but with sucrose solutions containing a buffer of 125 mM K_2SO_4, 10 mM morpholinopropanesulfonic acid (MOPS), pH = 6.8. The purified ROS were then washed in this buffer and passed through a 23-gauge needle. After soaking overnight in this buffer, the ROS were diluted (from a concentration of 10 mg rhodopsin/ml) into a buffer of 125 mM Na_2SO_4 and 10 mM MOPS, pH = 6.8, to obtain the appropriate transmembrane K+ gradient.

ROS suspensions were bleached either by continuous illumination or by a 600-μs duration flash delivered through a radiation window fitted to the electron spin resonance (ESR) cavity. Continuous illumination was provided by a 75-W high-pressure xenon arc lamp fitted with a heat filter (4 cm path of 0.5 M $CuSO_4$) and the desired interference filter. The arc lamp was sufficiently intense to bleach 100% of the rhodopsin contained in the ESR cell within several seconds. The 600-μs flash was provided by a xenon flash lamp fitted with a heat-absorbing glass filter (KG3-glass, Schott Inc., New York). The 100-J flash lamp input energy was sufficient to bleach ~50% of the rhodopsin contained in the ESR sample cell in a single flash.

RESULTS AND DISCUSSION

Spin Label I in ROS Membranes

An ESR spectrum of the spin-labeled phosphonium I in the presence of ROS disk membrane vesicles is shown in Fig. 1 and is very similar to those reported earlier for the phosphonium spin labels in egg phosphatidylcholine vesicles (Cafiso and Hubbell, 1978*a*). Such spectra are representative of two spin populations in slow exchange, one bound to the membrane and the other free in aqueous solution (Cafiso and Hubbell, 1978*a*). The line shape of the bound component indicates that the labels are not associated with rigid protein components in the membrane but rather are associated with fluid domains of the phospholipid bilayer.

The useful information contained in these composite spectra is the ratio of the bound-to-free spin populations. The procedure for extracting this quantity and its justification have been previously discussed (Castle and Hubbell, 1976). Briefly, the amplitude of the sharp,

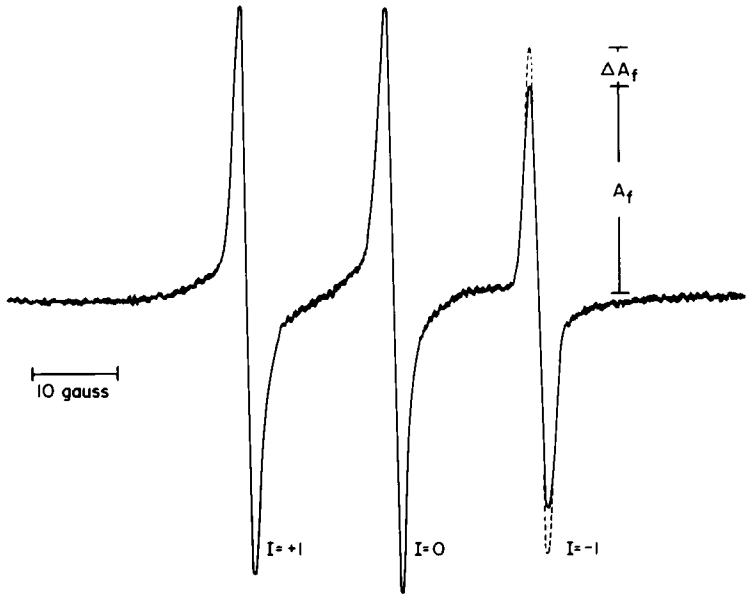

FIGURE 1 ERP spectrum of 2×10^{-5} M spin label I in the presence of ROS membranes (~ 2 mg rhodopsin/ml, 10 mM morpholinoethanesulfonic acid (MES), pH = 6.15). The spectrum is a superposition of spectra arising from bound and free populations. The dashed curve on the spin label I = −1 resonance shows the intensity of this line after a light flash bleaching the full complement of rhodopsin.

high field resonance in such composite spectra (that is the spin label I = −1 resonance, see Fig. 1) is dominated by the free spin component and thus affords a reasonable estimate of this population. Because little or no spin reduction occurs during the course of the experiments, the ratio of bound-to-free spins, λ, may be written as

$$\lambda = \frac{N_b}{N_f} = \frac{N_T - N_f}{N_f} = \frac{N_T}{N_f} - 1 \simeq \frac{A_T}{A_f} - 1, \tag{1}$$

where N_T, N_b, and N_f are the total number of moles of spin in the sample, the number of moles of membrane-bound spin and the number of moles of free spin, respectively. A_f is the amplitude of the positive branch of the high field resonance (Fig. 1) and A_T is the corresponding amplitude in the ESR spectrum of N_T moles of spin in the same buffer but in the absence of membranes. Changes in the bound-to-free spin ratio can be readily estimated as a function of time by recording just the peak amplitude of the high field resonance as a function of time and using Eq. 1 with known values of A_T. This procedure is reasonable for estimating bound-to-free ratios of spin labels I–V under the experimental conditions employed here where the bound signal amplitude is no > 5% of the total amplitude. Throughout this paper, we shall present experimental data in terms of $\Delta A_f/A_f$, the fractional change in the amplitude of the free spin signal (Fig. 1). When desired, this quantity may be used to compute the corresponding changes in λ according to Eq. 1.

Fig. 2 shows a recording of the positive branch of the high field resonance amplitude (A_f) of spin label I in a suspension of ROS membrane vesicles as a function of time before and after bleaching with continuous 533 nm radiation. There is a rapid increase in the amplitude of the

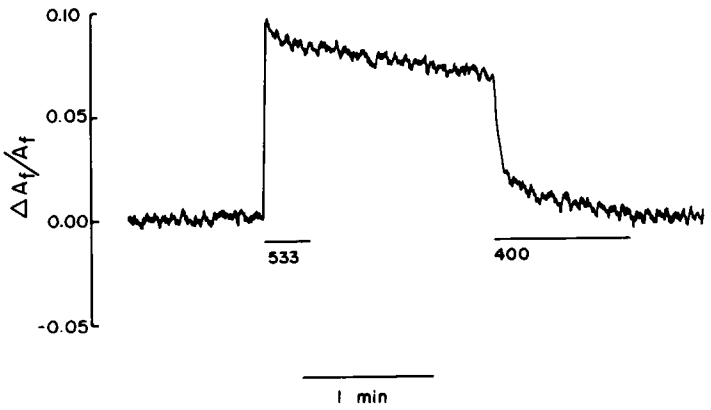

FIGURE 2 A recording of the amplitude of the free signal of spin label I as a function of time in the presence of ROS membrane vesicles (4 mg rhodopsin/ml, 10 mM MOPS, pH = 6.5). The amplitude changes are calibrated in terms of the fractional change $\Delta A_f/A_f$. The suspension was irradiated with either 533 or 400 nm light for a duration indicated by the length of the bar above the wavelength.

free signal upon bleaching which persists after the bleaching light is extinguished. A slow spontaneous decay in the amplitude is apparent after the initial rise, and shows first-order decay kinetics with a half-life of ~6 min at 20°C (Fig. 3). Irradiation of the bleached sample with 400 nm light before the spontaneous decay has completed causes a nearly complete reversal of the amplitude changes.

These light-dependent changes in the amplitude are the result of changes in the ratio of bound-to-free spin populations, i.e., the effective partition coefficient of spin label I between the aqueous phase and the ROS membranes is light-dependent. The light dependence of the partition coefficient apparently requires an intact membrane, since the disruption of the ROS membranes with either digitonin (1%) or Triton X-100 (0.2%) abolishes the light response.

The change in the partition coefficient is initiated by transformations in the rhodopsin molecule and is presumed to be associated with the appearance of one or more rhodopsin

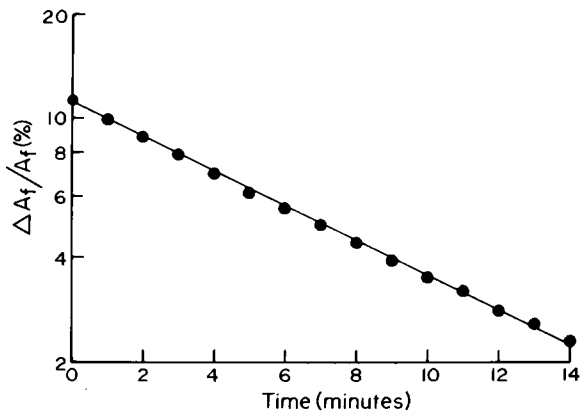

FIGURE 3 A plot of $\ln(\Delta A_f/A_f)$ vs. time after bleaching 100% of the rhodopsin with 533 nm light. The decay of the photoresponse is first order with a half-time of ~6 min. The ROS (4 mg rhodopsin/ml) were suspended in 10 mM MOPS, pH = 6.5.

conformers. The conformer(s) responsible for the observed effect must decay with a half-life of ~6 min, and the decay of the metarhodopsin II (MII) intermediate could be rate limiting (Kühn, 1978; Hoffmann et al., 1978). The amplitude of the response is a function of the amount of rhodopsin bleached and the bulk pH of the medium as shown in Fig. 4 and 5, respectively. The response amplitude is linear in the percent of rhodopsin bleached up to the maximum bleaching level investigated (50%). The pH dependence of the response suggests that the conformer(s) responsible is involved in a proton-dependent equilibrium with an effective pK_a of ~6.8. A simple quantitative explanation for the data in Fig. 4 and 5 is that $\Delta A_f/A_f$ is linearly related to the amount of a particular rhodopsin conformer, C_2, and that this conformer is in a proton equilibrium with at least one other form, C_1:

$$C_1 + H^+ \overset{K}{\rightleftharpoons} C_2. \tag{2}$$

In this situation, the pH dependence will be given by

$$\Delta A_f/A_f = \alpha \frac{K10^{-pH}}{1 + K10^{-pH}} \tag{3}$$

where α is the maximum value of $\Delta A_f/A_f$ at low pH and K is the equilibrium constant of reaction 2. The solid line in Fig. 5 is drawn according to Eq. 3 with $\alpha = 0.28$ and $K = 6.31 \times$

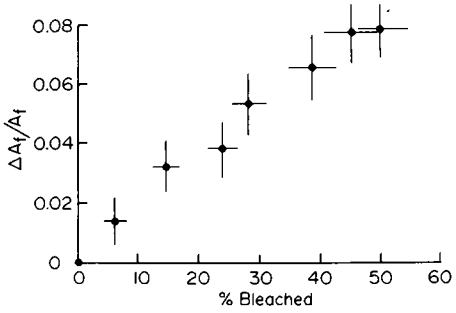

FIGURE 4

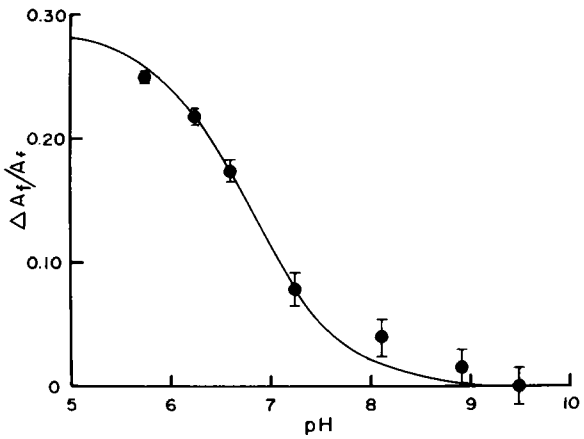

FIGURE 5

FIGURE 4 A plot of $\Delta A_f/A_f$ vs. the percent of rhodopsin bleached. The membrane suspension (4 mg rhodopsin/ml in 10 mM MES, pH = 6.15) was illuminated with a single flash (600 μs) from a xenon flash lamp. The amount of rhodopsin bleached in a single flash was varied by the use of neutral density filters located between the source and the sample. The extent of bleaching was determined by dissolving the ROS in 100 mM Tridecyltrimethyl ammonium bromide containing 0.1 M hydroxylamine and measuring the absorbance at 498 nm relative to that of the sample before bleaching.

FIGURE 5 A plot of $\Delta A_f/A_f$ vs. pH. The ROS (4 mg rhodopsin/ml) were bleached with continuous illumination so that 100% of the rhodopsin was bleached within a few seconds of illumination. The buffer was composed of 10 mM phosphate and 10 mM glycine adjusted to the appropriate pH. The points indicate the experimentally determined values of $\Delta A_f/A_f$ at various pH values and the solid line represents the best fit to the data as described in the text. The error bars represent error limits estimated on the basis of uncertainty in the measurement of ESR signal amplitudes.

10^6. Other more complex equilibria with several intermediates could also account for the data.

We have investigated the appearance kinetics of the response, and Fig. 6 shows the time-course of the amplitude of the high field resonance after a 600-μs xenon bleaching flash. The rise is exponential within experimental error with a half-time of 5 ms at 23.3°C. The temperature dependence of the rate constant for appearance has been investigated at pH = 5.5 and the data are presented as an Arrhenius plot in Fig. 7. The activation energy determined from the slope is 27 ± 2 kcal/mol.

The time-course of the response certainly places the generator conformer (C_2) within the time domain usually associated with the appearance of MII (Abrahamson, 1973; Applebury et al., 1974; Williams, 1975; Stewart et al., 1977; Hoffmann et al., 1978; Rapp, 1979). The pH dependence and activation energy also resemble those reported for the appearance of MII (Matthews et al., 1963; Pratt et al., 1964; Sengbusch and Stieve, 1971; Applebury et al., 1974; Williams, 1975; Stewart et al., 1977; Hoffmann et al., 1978; Rapp, 1979). In addition, the thermal decay of the response (Fig. 3) is similar to the decay of MII (Kühn, 1978; Hoffmann et al., 1978). The rapid disappearance of the response upon irradiation at 400 nm (Fig. 2) is also consistent with a MII decay-limited process, because MII is converted to other intermediates when irradiated near its broad absorption maximum at 380 nm (Williams, 1975). Finally, it should be noted that the presence of 0.2 M hydroxylamine in the membrane suspension (at pH = 6.8) greatly diminishes the light-dependent partitioning of spin label I.

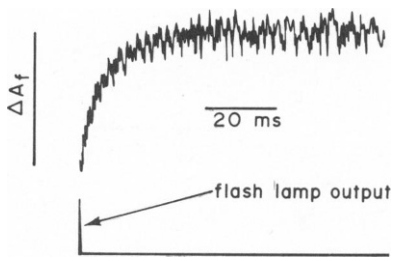

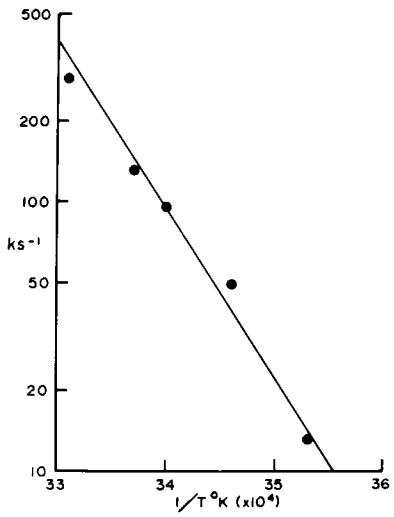

FIGURE 6

FIGURE 7

FIGURE 6 A recording of ΔA_f, the change in free signal intensity of spin label I in an ROS suspension (4 mg rhodopsin/ml, 1 mM MES, pH = 5.5) following a 600- μs flash (white) from a xenon flash lamp. The flash lamp duration is indicated below the trace and bleached slightly < 50% of the rhodopsin present; the rise of the signal is exponential (within experimental error) and has a half-time of ~5 ms at 23.3°C.

FIGURE 7 An Arrhenius plot of the rate constant, k, for the appearance of ΔA_f after a 600- μs flash. ROS were at a concentration of 4 mg rhodopsin/ml in 1 mM MES, pH = 5.5. The activation energy for the rate limiting process leading to ΔA_f is 27 ± 2 kcal/mol.

This is consistent with MII decay as a rate limiting step in the decay of the response since hydroxylamine rapidly cleaves the linkage between opsin and retinal in MII. The metarhodopsins mentioned above are traditionally defined on the basis of their spectral absorption maxima, but recently evidence has been presented which suggests the existence of isochromic forms of both metarhodopsin I (MI) and MII (Williams; 1975; Emrich and Reich, 1976; Bennett, 1978). Thus, the spectrally defined intermediates may each have several distinct conformational forms, and we will not attempt a detailed identification of the generator conformation(s) with the spectrally defined intermediates.

Origin of the Photoresponse

As mentioned in the introduction, there is substantial evidence that hydrophobic ions like spin label I bind to bilayer membranes at potential minima located near the interfaces but within the low dielectric interior of membranes (Fig. 8 *a*). The positions of these minima define the

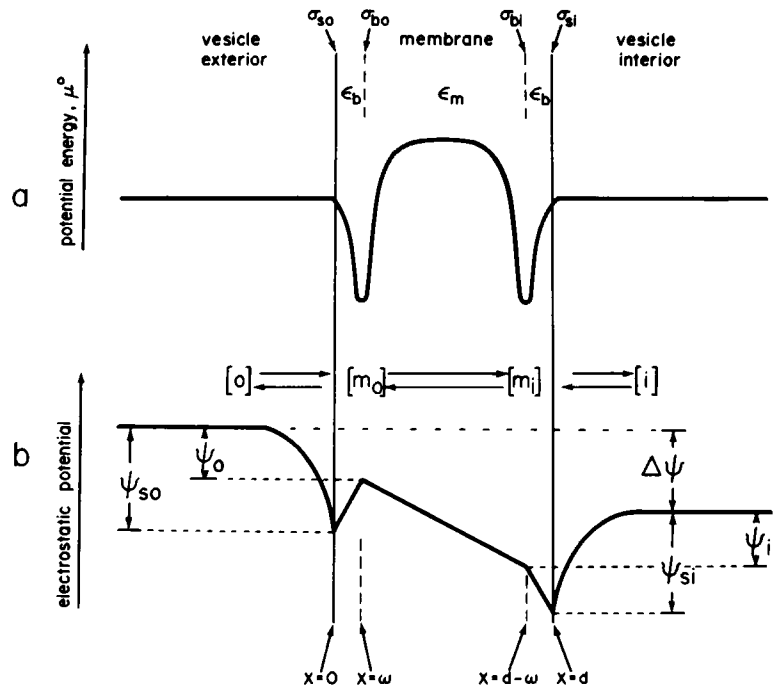

FIGURE 8 (*a*) The standard state chemical potential profile across a thin hydrocarbon slab of thickness d for a hydrophobic ion in the absence of any electric potential differences (from Ketterer et al., 1971). The deep minima at $x = \omega$ and $x = d - \omega$ define the "boundary regions" labeled m_o *and* m_i. ϵ_m is the dielectric constant of the membrane hydrocarbon interior, and ϵ_b is the dielectric constant of the interfacial region between $x = 0$ and $x = \omega$ and the corresponding region of the opposite interface. (*b*) A general electrostatic potential profile across the membrane showing several possible interfacial and transmembrane components. ψ_i and ψ_o are the internal and external boundary potentials (see footnote 7), ψ_{so} and ψ_{si} are the external and internal surface potentials and $\Delta\psi$ is the transmembrane potential. The boundary potentials may differ from the surface potentials as a result of intramembrane dipoles or net charge density in or near the boundary region. Note that the boundary potentials are the sum of a surface potential and the potential difference from the surface to the boundary region. σ_{bo} and σ_{bi} are the charge densities in the planes defined by the potential energy minima shown in (*a*) at $x = \omega$ and $x = d - \omega$. σ_{so} and σ_{si} are the charge densities at the membrane outer and inner surfaces.

membrane boundary regions. We assume that the potential barrier within the membrane proper is sufficiently high to prevent significant accumulation of spin label I in this region. Thus at equilibrium, appreciable concentrations of spin label I would be found only in the four discrete regions of space labeled o, m_o, m_i, and i corresponding to the external aqueous space surrounding the vesicle, the outer boundary region, the inner boundary region and the interior aqueous volume of the vesicle respectively. This model for the equilibria of spin label I are discussed in more detail by Cafiso and Hubbell (1978*a*). The molecules of spin label I occupying regions m_o and m_i are considered "bound" and those in o and i are "free." The distribution of spin label I among these various regions, and thus the bound-to-free ratio, depends on the relative standard-state chemical potentials as well as any electrostatic potentials. In an earlier publication (Cafiso and Hubbell, 1978*a*), it was shown that the ratio of bound-to-free spin populations (λ) of the phosphoniums in the presence of closed vesicles can be analytically expressed as

$$\lambda = \frac{V_{m_i}}{V_i} \frac{K'_{m_i} e^{-\psi_i ZF/RT} + K'_{m_o} \frac{V_{m_o}}{V_{m_i}} e^{-\psi_o ZF/RT} \cdot e^{\Delta\psi ZF/RT}}{1 + \frac{V_o}{V_i} e^{\Delta\psi ZF/RT}}, \tag{4}$$

where V_o, V_i, V_{m_o}, and V_{m_i} are the effective volumes per vesicle of the four regions of space o, i, m_o, m_i, respectively and K'_{m_i}, K'_{m_o} are the binding constants of spin label I to the inner and outer potential minima in the absence of electrostatic potentials. The various electrostatic potentials in Eq. 4 are defined in Fig. 8 *b* which shows a general electrostatic potential profile which might exist across a membrane with surface, boundary, and transmembrane potential differences. It is apparent from Eq. 4 and Fig. 8 *b* that changes in the surface potentials ψ_{so} or ψ_{si}, the boundary potentials[2] ψ_o or ψ_i, the transmembrane potential, or the zero potential binding constants will all lead to changes in λ, and each or all could be responsible for the observed light-dependent changes seen in the ROS vesicles. Fortunately, it is possible to systematically investigate each possibility.

Consider first changes in K'_{m_i}, K'_{m_o}. Nonelectrostatic physical changes in the membrane bilayer would be expected to produce changes in these binding constants and thus changes in λ. Changes in bilayer fluidity would be an example. Such changes should also be reflected in changes of the partitioning or mobility of an uncharged hydrophobic spin label such as 2,2,6,6-tetramethylpiperidine-1-oxyl (TEMPO) or spin label V. However, we find that both the partition coefficients and mobilities are unchanged upon bleaching with continuous 533-nm illumination for either of these labels in the presence of ROS membrane vesicles (data not shown).[3] Thus, it is considered very unlikely that the changes shown in Fig. 1 result from

[2]McLaughlin (1977) and Andersen et al. (1978) define the boundary potential to be the potential at $x = \omega$ (or $x = d - \omega$) relative to the surface potential. In the present paper, the boundary potential refers to the potential at $x = \omega$ (or $x = d - \omega$) relative to the bulk aqueous medium. The difference is thus one of reference state. The above choice for the reference state is convenient here since the phosphonium equilibria directly give the potential at $x = \omega$ relative to the bulk aqueous phase.

[3]Verma et al. (1973) observed a slight decrease in rotational correlation time for the stearic acid derivative of spin label V in ROS membranes upon complete bleaching. This would imply an increase in fluidity of the membrane which in turn is expected to increase the partition coefficient of hydrophobically associated molecules. In addition, Pontus and Delmelle (1975) observed an increase in the binding of TEMPO to ROS membranes upon bleaching. We

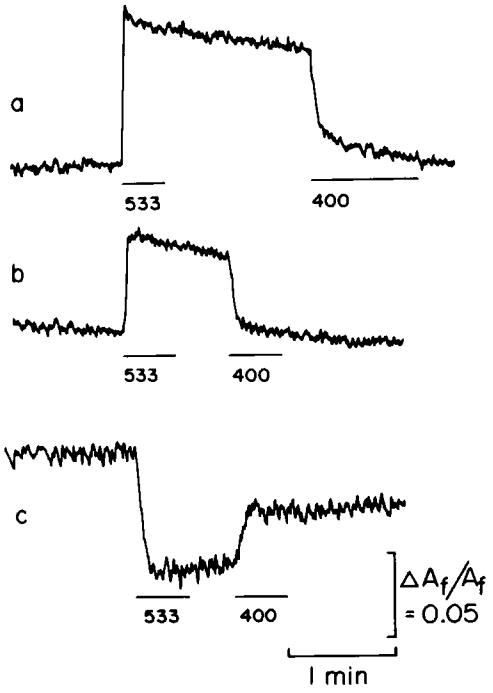

FIGURE 9

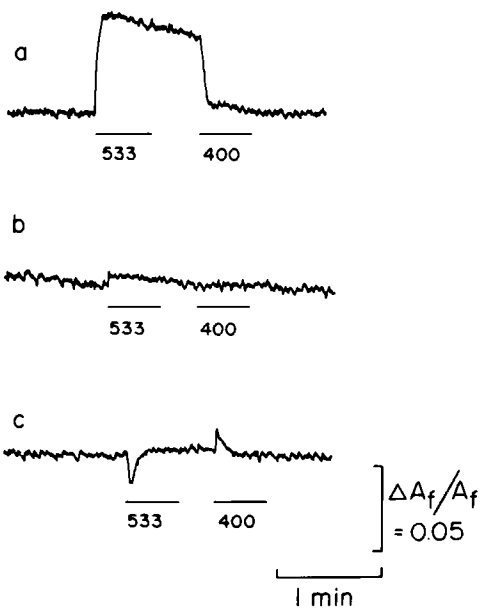

FIGURE 10

FIGURE 9 Recordings of $\Delta A_f/A_f$ while irradiating the ROS membranes (4 mg rhodopsin/ml) in low salt (1 mM MOPS, pH = 6.5) for several different spin labels each at a concentration of ~35 μM. (*a*) Spin label I, the phosphonium label; (*b*) spin label II, the quaternary ammonium label which responds exclusively to changes in the surface potential; (*c*) spin label IV, a negatively charged sulfate label which is also sensitive only to surface potentials. The ROS were irradiated with illumination at 533 or 400 nm for times indicated by the length of the bars above the wavelengths.

FIGURE 10 Changes in $\Delta A_f/A_f$ while irradiating ROS membranes (4 mg rhodopsin/ml) in high salt (100 mM NaCl, 1 mM MOPS, pH = 6.5) for several different spin labels each at a concentration of ~35 μM. (*a*) Spin label I, the phosphonium label; (*b*) spin label II, the ammonium label; (*c*) spin label III, the secondary amine which is sensitive to ΔpH. This sample was washed and suspended in 500 mM NaCl rather than 100 mM salt to minimize any small effects due to surface potential changes. The ROS were irradiated with illumination at 533 or 400 nm for times indicated by the length of the bars above the wavelengths.

changes in the K's. Changes in the transmembrane potential are apparently not responsible for the changes in $\Delta A_f/A_f$ shown in Fig. 2 since the addition of valinomycin (10 μM), nonactin (10 μM), or carbonylcyanide *m*-chlorophenylhydrazone (CCCP [10 μM]) either alone or in any combination has no effect on the light response.

Changes in surface potentials are readily investigated using spin labels II and IV, which have been shown to be useful in the estimation of surface potentials in phospholipid vesicles (Castle and Hubbell, 1976; Gaffney and Mich, 1976; Melhorn and Packer, 1976). As a result

do not at this time understand the reasons for the difference between these results and ours, but it is important to note that the effects observed by these authors cannot be related to the phosphonium bleaching response since they are in the opposite direction.

of the high charge density of the ionic moiety of these labels, the charge centers cannot enter the low dielectric regions occupied by the phosphoniums. Thus, these molecules sense electrostatic potential changes exclusively at the membrane-solution interface. Fig. 9 *b* shows the response of spin label II to a bleaching light in the presence of ROS vesicles under low ionic strength conditions where the surface potential effects are maximal. Fig. 9 *a* shows the response of spin label I for comparison under the same ionic strength conditions. Clearly the changes sensed by spin label II are similar to those sensed by spin label I under these conditions. Furthermore, the time-course of the response of label (II) to a 600-μs bleaching flash is identical (within experimental error) to that of spin label I shown in Fig. 6. Fig. 9 *c* shows the response of spin label IV to a bleaching light. The opposite response of this negatively charged label compared to the positively charged spin label II strongly argues that the changes observed are electrostatic in origin. Thus, under low ionic strength conditions, the light-induced changes in the ROS membranes are reflected in the modulation of electrostatic potential at the membrane-solution interface. Fig. 10 shows the response of spin labels I and II under high salt conditions. As can be seen in Fig. 10 *b*, the changes in surface potential are screened at high ionic strengths, i.e., the light-dependent modulation of the surface potential as sensed by spin label II is nearly absent. However, under the same high ionic strength conditions, the response reported by spin label I is only slightly diminished (Fig. 10 *a*). This implies that spin label I senses changes in electrostatic potentials which cannot be screened by high salt concentration and therefore spin label I cannot be responding to changes in charge density at the membrane surface alone. The above data strongly suggests that the origin of the changes in λ lies in the modulation of the electrostatic potentials in the low dielectric boundary regions near $x = \omega$ or $x = d - \omega$ (Fig. 8) or both, and henceforth we assume that the absorption of a photon by rhodopsin produces an increase in an electrostatic boundary potential within ROS membranes, a potential physically distinct from the surface potential. The potential in the boundary region must increase rather than decrease since the binding of the positively charged phosphonium decreases.

Although the photoresponse of spin label I cannot be abolished at high salt concentration it is definitely reduced in amplitude. Fig. 11 shows the dependence of $\Delta A_f/A_f$ on NaCl concentration at low pH. The origin of the salt dependence will be discussed below.

Proton Uptake

In the first part of this paper, evidence was presented to indicate that the change in boundary potential was coincident with the appearance of a protonated species of bleached rhodopsin. Because the illumination of ROS disks is accompanied by the uptake of protons (McConnell et al., 1968), an instantaneous pH gradient may be generated across the disk membrane vesicles in the absence of strong buffering capacity. Earlier, it was shown that spin label III can be used to determine transmembrane pH gradients across sealed vesicles, and we have employed this method here (Cafiso and Hubbell, 1978 *b*). Fig. 10 *c* shows a recording of the peak of the high field resonance of spin label III in the presence of ROS vesicles and at a salt concentration sufficiently high to suppress small changes due to surface potential effects. It can be seen that the bound-to-free ratio of this label increases rapidly upon bleaching and then quickly decays. This response indicates the rapid creation and decay of a pH gradient, outside basic, across the vesicle upon bleaching. Illumination of the *bleached* membranes at 400 nm (Fig. 10 *c*) causes a reverse gradient to build-up (inside basic). In either case, the rather rapid

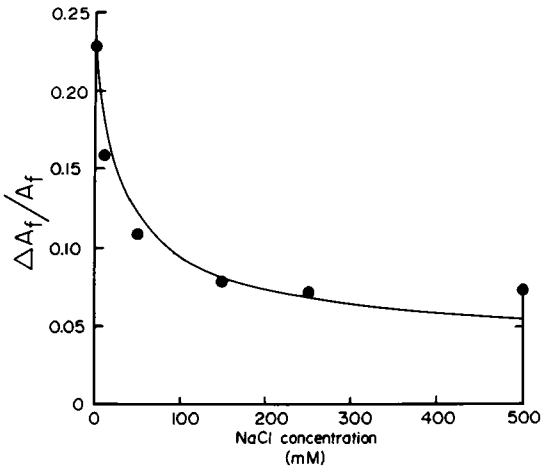

FIGURE 11 A plot of the dependence of $\Delta A_f/A_f$ upon the monovalent salt concentration. The points (●) are the experimentally determined values of $\Delta A_f/A_f$ for label (I) after bleaching 100% of the rhodopsin present with 533-nm illumination (the ROS suspension contained 4 mg rhodopsin/ml in1 mM MES pH – 5.5 with various concentrations of NaCl). The solid line is the calculated dependence of $\Delta A_f/A_f$ upon salt concentration from the model and parameters given in the text.

decay of the gradient after its initial build-up is attributed to a finite proton permeability of these vesicles. The addition of (10 μm) CCCP or the presence of a moderate buffer (e.g. 10 mM MOPS) eliminates the responses to illumination as measured by spin label III. Measurements in these same preparations with a pH electrode show an increase in external pH upon illumination at 533 nm which persists long after ΔpH has decayed (many minutes). Illumination at 400 nm causes a drop in the external pH. These responses are not affected by CCCP. These results are consistent with the idea that proton uptake and release on the external surface of the vesicles are responsible for the changes seen in ΔpH with 533- and 400-nm illumination, respectively; proton movement across these vesicles upon illumination cannot account for these results.

Photoresponses in Fresh Membranes

All of the results presented above were obtained using membranes prepared from frozen retinas. Membranes prepared from "fresh" retinas obtained within a few hours of slaughter also show bleaching responses measured by spin label I, but with the interesting differences shown in Fig. 12. With fresh membranes, ~50% of the initial amplitude decays rapidly with the remainder decaying at the same rate as the response from membranes prepared from frozen retinas (Fig. 12 *a*). In the presence of 10 μM valinomycin or 10 μM nonactin the response is identical to that seen in membranes from frozen retinas (Fig. 12 *b*).

The effect of ionophores indicates that this additional rapidly decaying component is related to changes in *transmembrane potential.* From the dependence of λ on $\Delta\psi$ given by Eq. 4 we conclude that the ionophore-sensitive component which accounts for 50% of the initial amplitude upon bleaching most likely arises from an inside positive transmembrane potential. The decay of the transmembrane potential is attributed to the finite ion permeability of the membranes.

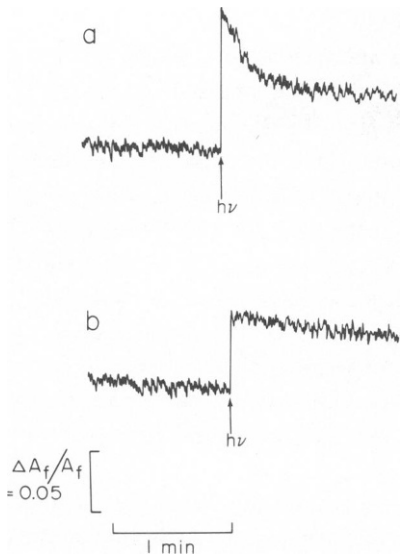

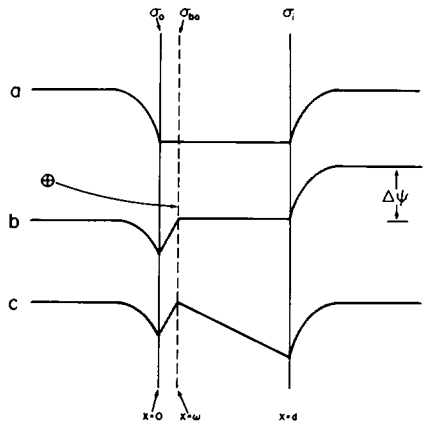

FIGURE 12

FIGURE 13

FIGURE 12 Recordings of $\Delta A_f/A_f$ for spin label I in the presence of ROS membrane vesicles isolated from "fresh" retinas as described in the experimental section. The ROS are suspended in 125 mM K_2SO_4, 10 mM MES, pH = 6.15, and bleached with a 600- μs duration xenon flash. (*a*) Without valinoycin and (*b*) in the presence of 10 μM valinomycin.

FIGURE 13 Simplified electrical potential profiles across a membrane. The membrane-solution interfaces are at $x = 0$ and $x = d$, and $x = \omega$ defines the external boundary region. (*a*) Completely symmetric membrane with boundary potentials equal to the surface potentials. The surfaces have charge densities of σ_{so} and σ_{si}. The charge density in the boundary region, σ_{bo}, is zero. (*b*) Immediately after an increase in external boundary potential. In this example, the boundary potential is increased due to an increase in σ_{bo}. An instantaneous transmembrane potential, $\Delta\psi$, is created. (*c*) The profile after the relaxation of $\Delta\psi$. Due to the finite membrane permeability, ionic currents discharge the membrane capacitance.

The observation of the transmembrane potential transient is of particular importance here because the generation of a transmembrane potential is expected to accompany a change in boundary potential only if the change in boundary potential is asymmetric. This is indicated graphically in Fig. 13 *a* and *b* which show a simplified electric potential profile across a membrane before and immediately after an increase in the external boundary potential. Notice that this produces an inside positive transmembrane potential as experimentally observed. A symmetric increase in the boundary potential would clearly produce no transmembrane potential. An increase in the internal boundary potential would produce an inside negative transmembrane potential which is contrary to experimental observation. Thus we conclude that the light-induced increase in boundary potential occurs at the external (cytoplasmic) surface of the disk membrane. The finite ion permeability of the ROS disk membranes results in a current and a decay in the transmembrane potential. In Fig. 13 *c* the electric profile across the membrane after the decay of the transmembrane potential is depicted.

The fact that no transmembrane potential transients are observed with frozen-thawed membrane preparations is almost certainly due to the high ionic permeability of these membranes. In this case, $\Delta\psi$ would decay faster than the measurement could resolve.

A Model for the Photoresponse

At this point, it will be helpful to summarize the results and formulate a specific model for the photoresponse. The following features are suggested by the results presented above: (*a*) The light-dependent changes in the partition coefficient of spin label are due to a light-dependent change in an electrostatic potential in the membrane. This photopotential is somewhat reduced but cannot be abolished at high salt concentrations and is associated with a region of space within the bilayer inaccessible to salts in the aqueous medium. (*b*) A photopotential is also detected by spin label II which senses electrostatic potentials only at the membrane-solution interface (surface potentials). This potential, unlike that sensed by spin label I, is abolished at high salt concentrations. (*c*) The time-courses of the light-induced signals obtained from spin labels I and II are identical within experimental error. (*d*) The boundary potential increase sensed by spin label I is asymmetric, with an increase in potential at the external (cytoplasmic) boundary region relative to the internal boundary region. Proton uptake also occurs at this surface.

The simplest process that will readily account for these observations is an interfacial charge translocation across the external membrane surface; the net result is the translocation of positive charge from the aqueous solution to a boundary region in the membrane.[4] The increase in positive charge density results in an increase in boundary potential in the region near $x = \omega$ (Fig. 13) which in turn decreases the partition coefficient of spin label I. The charge placed in the low dielectric near $x = \omega$ will also produce a potential at the membrane-solution interface which will be sensed as a salt-dependent surface potential by spin label II. This model accounts for the fact that the time-course of the potentials sensed by spin labels I and II are the same, in addition to the fact that the photopotential sensed by spin label II is abolished by salt while that sensed by spin label I is not. Since one component of the boundary potential, the surface potential, is salt-dependent, the model readily accounts for the salt dependence of $\Delta A_f/A_f$ for spin label I given in Fig. 11. This will be discussed in more detail below.

It is conceivable that the boundary potential sensed by spin label I arises as a result of a dipole creation or reorientation within the membrane. This possibility cannot be excluded, but it seems unlikely that a membrane dipole could give rise to a strongly salt-dependent surface potential (McLaughlin, 1977; Trissl, 1979). To develop a convincing dipole model, one would have to assume that the potentials sensed by spin labels I and II have independent origins, and there is at present no experimental evidence to suggest that this is the case. Thus, we tentatively adopt the interfacial charge translocation model as the most reasonable representation of the process which gives rise to the photopotentials.

It is of interest at this point to obtain an estimate for the actual amount of charge that would have to be translocated to the boundary region per photoactivated rhodopsin molecule to account for the observed values of $\Delta A_f/A_f$. We have approached this problem by calculating theoretical values of $\Delta A_f/A_f$ as a function of charge density in the boundary layer.[5] This semiquantitative calculation also serves to reveal further details of the model and is outlined below.

---

[4]In principle, we cannot distinguish between the translocation of positive charge into the membrane and the translocation of negative charge from the membrane to the aqueous phase.

[5]Within the context of the interfacial charge translocation model, there is no *a priori* reason to expect the charge to be

Because we are interested in light-dependent changes, the potentials ψ_o and ψ_i in Eq. 4 will be written as $\psi_o = \psi_o^d + \psi_o^\ell$, and $\psi_i = \psi_i^d + \psi_i^\ell$, where superscript d refers to the component of the potential present in the dark and the superscript ℓ refers to the light-dependent increment in the potential. For simplicity, we incorporate the dark components into the binding constants and define, $K_{m_i} = K'_{m_i} e^{-\psi_i^d ZF/RT}$ $K_{m_o} = K'_{m_o} e^{-\psi_o^d ZF/RT}$. The bound-to-free ratio of spin label I after a flash (λ^ℓ) may then be written in terms of light-dependent quantities as:

$$\lambda^\ell = \frac{V_{m_i}}{V_i} \cdot \frac{K_{m_i} e^{-\psi_i^\ell ZF/RT} + \frac{V_{m_o}}{V_{m_i}} K_{m_o} e^{-\psi_o^\ell ZF/RT} \cdot e^{\Delta\psi ZF/RT}}{1 + \frac{V_o}{V_i} e^{\Delta\psi ZF/RT}}. \tag{5}$$

Because the transmembrane potential ($\Delta\psi$) is zero in the dark-adapted membrane, the bound-to-free ratio in the dark, λ^d, is simply:

$$\lambda^d = \frac{V_{m_i}}{V_i} \frac{K_{m_i} + \frac{V_{m_o}}{V_{m_i}} K_{m_o}}{1 + \frac{V_o}{V_i}}. \tag{6}$$

In terms of λ^ℓ and λ^d,

$$\frac{\Delta A_f}{A_f} = \frac{\lambda^d + 1}{\lambda^\ell + 1} - 1. \tag{7}$$

To compute values of $\Delta A_f / A_f$ according to Eq. 5–7, the potentials ψ_o^ℓ, ψ_i^ℓ, and $\Delta\psi$ are required and are calculated on the basis of the simple electrostatic model of the membrane shown in Fig. 8 *b*. This model is essentially the "three capacitor" model used by Andersen et al. (1978) in describing boundary potentials due to the absorption of tetraphenylboron to bilayers. We make the drastic simplification that all charges are smeared uniformly over the surface on which they are located. In addition, we limit our calculations to situations where the interfacial charge translocated per unit area of membrane is small compared to the fixed surface charge density. As will be shown below, this situation pertains to the ROS membranes and permits the surface potentials after charge translocation to be approximated by the truncated Taylor series,

$$\psi_s \simeq \psi_s^d + \left(\frac{\partial\psi_s}{\partial\sigma}\right)\sigma_b^\ell,$$

where ψ_s^d and ψ_s are the surface potentials before and after interfacial charge translocation, respectively, and σ_b^ℓ is the light-induced change in the charge density of the boundary layer.

translocated to the particular boundary region defined by the phosphonium potential minimum. In the calculations, we have taken this to be the case. Assuming all other features of the model are correct, the calculation will thus yield the minimum number of charges translocated per rhodopsin if the charge is placed at $x < \omega$ and the correct number if at $x \geq \omega$ (Fig. 8). Considering that ω is on the order of 2 Å, it is unlikely that the charge could be placed at a distance significantly less than ω, and taking the charge to be placed at $x = \omega$ is not intolerable for an approximate calculation.

Making use of this expansion for the surface potentials and Gauss' theorm, the desired potentials are obtained in terms of light-induced charge densities as:

$$\psi_o^{\ell} = \left(\frac{\partial \psi_{so}}{\partial \sigma_{so}}\right) \sigma_{bo}^{\ell} + \frac{\omega}{\epsilon_b \epsilon_o} [\sigma_{bo}^{\ell} - \sigma_o'] \tag{8}$$

$$\psi_i^{\ell} = \left(\frac{\partial \psi_{si}}{\partial \sigma_{si}}\right) \sigma_{bi}^{\ell} + \frac{\omega}{\epsilon_b \epsilon_o} [\sigma_{bi}^{\ell} - \sigma_o'] \tag{9}$$

$$\Delta\psi = \left(\frac{\partial \psi_{so}}{\partial \sigma_{so}}\right) \sigma_{bo}^{\ell} - \left(\frac{\partial \psi_{si}}{\partial \sigma_{si}}\right) \sigma_{bi}^{\ell} + \frac{\omega}{\epsilon_b \epsilon_o} (\sigma_{bo}^{\ell} - \sigma_{bi}^{\ell}) - \frac{2\sigma_o'}{\epsilon_o} \left[\omega \left(\frac{1}{\epsilon_b} - \frac{1}{\epsilon_m}\right) + \frac{d}{2\epsilon_m}\right]. \tag{10}$$

In these expressions, σ_{bo}^{ℓ} and σ_{bi}^{ℓ} are light-induced changes in charge density at the outer and inner boundary layers at $x = \omega$ and $x = d - \omega$, respectively. The potentials ψ_{so} and ψ_{si}, the distances ω and d, the charge densities σ_{so} and σ_{si} and the dielectric constants ϵ_m and ϵ_b are those defined in Fig. 8.

The quantity σ_o' is essentially defined by Eq. 10 and is the excess external membrane surface charge density arising from ion flow across the membrane induced by the photopotentials. In Eqs. 8–10, $\sigma_o' = 0$ at the instant of interfacial charge translocation and $\Delta\psi$ is given by Eq. 10 with $\sigma_o' = 0$. After the relaxation of $\Delta\psi$ due to transmembrane ion flow, σ_o' is given by Eq. 10 with $\Delta\psi = 0$.

Eqs. 5–10 provide the means for computing values of $\Delta A_f/A_f$, the experimentally determined quantity, for arbitrary values of σ_{bo}^{ℓ} and σ_{bi}^{ℓ}. We now consider application of this general theory to the specific model of interfacial charge translocation outlined above. Since the specific model being considered involves interfacial charge transfer at the external membrane surface only, we take $\sigma_{bi}^{\ell} = 0$. Assuming that each photoactivated rhodopsin contributes z elementary charges to the boundary layer at the surface,

$$\sigma_{bo}^{\ell} = \rho_s f z, \tag{11}$$

where f is the fraction of rhodopsin photoactivated and ρ_s is the known surface density of rhodopsin in the ROS membranes. In principle, we are now in a position to compute values of $\Delta A_f/A_f$ as well as the various potentials as a function of f for any value of z.

To carry out the calculation, it is first necessary to obtain numerical values for the various constants appearing in Eqs. 5 and 6. Freeze-fracture electron micrographs of ROS membrane vesicles prepared according to procedures used here indicate a spherical shape with an average radius of $r \simeq 0.25$ μm.[6] Norisuye et al. (1976) have obtained the same value from quasielastic light-scattering studies of ROS vesicles. For these large spherical vesicles, we expect $V_{m_o}/V_{m_i} \simeq 1$ (Cafiso and Hubbell, 1978*a*), and for a rhodopsin surface density of 2×10^4 rhodopsins/μm^2 (Chen and Hubbell, 1973), V_o/V_i is readily estimated as:

$$\frac{V_o}{V_i} \simeq \frac{1}{r[\text{rho}]} - 1, \tag{12}$$

where r is the vesicle radius in Å and [rho] is the molar concentration of rhodopsin in the vesicle suspension.

---

[6]Cafiso, D. S., and W. L. Hubbell. Unpublished observations.

At the present time, we have not been able to independently measure K_{m_o} and K_{m_i}, the binding constants of spin label I to the two membrane surfaces. However, an estimate of the ratio of these binding constants can be obtained in the following way. Using procedures described in the experimental section, K+ diffusion potentials have been established across dark-adapted ROS vesicles with valinomycin in the presence of known K+ ion gradients across the membrane. In this situation the λ of spin label I will be given by Eq. 4 with $\psi_i, \psi_o = 0$ and with $\Delta\psi$ equal to the K+ diffusion potential. When a gradient of K+ was established across dark ROS vesicle membranes so that K+in/K+out $\simeq 5$, the experimental value of λ differed from that predicted by Eq. 4 by only 15% when $\Delta\psi$ was taken as -40 mV (the K+ diffusion potential)[7] and K_{m_o} was assumed to be equal to K_{m_i}. This empirical calibration approach suggests that the two binding constants are of similar magnitude, and we may take $K_{m_i} \approx K_{m_o} \equiv K$ for the purposes of an approximate calculation. With the above reasonable approximation, λ^ℓ and λ^d take the particularly simple forms:

$$\lambda^d \simeq \frac{KV_{m_i}}{V_i} \frac{2}{1 + \dfrac{V_o}{V_i}} \tag{13}$$

$$\lambda^\ell \simeq \frac{KV_{m_i}}{V_i} \frac{1 + e^{-\psi_o^\ell ZF/RT} \cdot e^{\Delta\psi ZF/RT}}{1 + \dfrac{V_o}{V_i} e^{\Delta\psi ZF/RT}}. \tag{14}$$

Using experimental values of λ^d determined directly from the ESR spectra and V_o/V_i calculated according to Eq. 12, a value for KV_{m_i}/V_i is obtained from Eq. 13. This is a constant of the vesicle preparation and is used in the calculation of λ^ℓ according to Eq. 14. To compute values of λ^ℓ for various values of σ_{bo}^ℓ immediately after the flash, ψ_o^ℓ and $\Delta\psi$ are evaluated with $\sigma_o' = 0$ using Eq. 8–10, and λ^ℓ and $\Delta A_f/A_f$ are then found from Eqs. 14 and 7, respectively. Values of $\Delta A_f/A_f$ following the decay of the transmembrane potential are found by setting $\Delta\psi = 0$ in Eq. 10 and solving for σ_o'. Using this value, ψ_o^ℓ and ψ_i^ℓ are evaluated from Eq. 8–10 and the remainder of the calculation is carried out as above. For the calculation of ψ_o^ℓ according to Eq. 8 the partial $(\partial\psi_{so}/\partial\sigma_{so})$ is obtained from the Gouy-Chapman equation which has been found to adequately represent membrane surface potentials as a function of both salt concentration and charge density (McLaughlin, 1977). To obtain numerical values for the partial derivative, the membrane external charge density must be known. This has been estimated as $\sigma_{so} \approx -2.7 \times 10^{-2}$ C/m^2 according to published procedures (Castle and Hubbell, 1976). Details of these experiments will be published elsewhere. Because $\sigma_{bi}^\ell = 0$ in the model, $(\partial\psi_{si}/\partial\sigma_{si})$ need not be evaluated. Eqs. 8–10 also require a knowledge of the distances d and ω and the dielectric constants ϵ_m and ϵ_b. The membrane hydrophobic thickness, d, is taken as 50 Å. In an earlier work, ω was estimated as having a maximum value of $\simeq 2$ Å (Cafiso and Hubbell, 1978*a*) and that is the value used in the present calculation. This is not at odds with other estimates of ω (Andersen et al., 1978; Tsien, 1978). The dielectric of the membrane interior, ϵ_m, is taken to be 2. There is no precedent for assigning a value for ϵ_b. In the idealized hydrocarbon slab model for the membrane, ϵ_b would be 2. In reality, this interfacial region

[7] -40 mV is the value of the K+ diffusion potential calculated from the Nernst equation assuming that PK+>>> PSO_4^-, PNa+. In the presence of valinomycin, this is assumed to be the case in the ROS membranes.

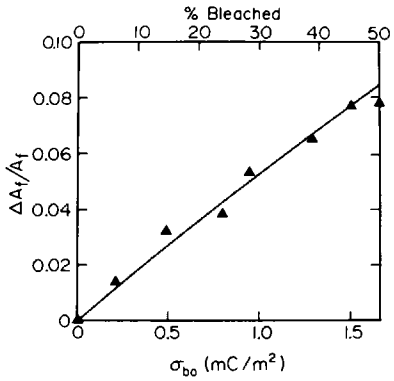

FIGURE 14 The dependence of $\Delta A_f/A_f$ upon σ_{bo}^{ℓ} calculated as described in the text for membranes suspended in 0.11 M salt (—) and assuming each photoactivated rhodopsin contributes one elementary charge to σ_{bo}^{ℓ}. The points (Δ) are the experimentally determined values $\Delta A_f/A_f$ from Fig. 4 plotted as a function of the percent of rhodopsin bleached. Rigorously, the figure should compare the calculated value of $\Delta A_f/A_f$ as a function of σ_{bo}^{ℓ} with the experimental result in terms of the fraction of total rhodopsin in the protonated form rather than the fraction of rhodopsin bleached. The two quantities are the same only at low pH. At a pH of 6.15, where the data of Fig. 4 were collected, ~80% of the bleached protein is in the protonated form and the approximate nature of the calculation presented does not warrant the correction. Considering the various uncertainties, it would appear that between 0.5 and 2 charges are required per M II formed.

should be penetrated by water to some degree and presumably contains some polar groups of the lipid molecules, perhaps the glycerol backbone (Levine et al., 1979). Thus ϵ_b should be somewhat larger than 2 and we have taken $\epsilon_b \approx 6$ as a reasonable estimate consistent with the capacitance of the outer boundary region (Andersen et al., 1978).

Fig. 14 shows the expected dependence of $\Delta A_f/A_f$ (after relaxation of $\Delta\psi$) on σ_{bo}^{ℓ} as predicted by the model for a salt concentration of 0.11 M. The dependence is essentially linear, just as the dependence of $\Delta A_f/A_f$ on the fraction of rhodopsin bleached (Fig. 4). The experimental and theoretical values of $\Delta A_f/A_f$ are in close agreement if it is assumed that each photoactivated rhodopsin contributes approximately one elementary charge in the vicinity of $x = \omega$, that is if $z \approx 1$ in Eq. 11. This correspondence is indicated in Fig. 14 by replotting the data of Fig. 4 using the upper axis to represent the percent bleaching corresponding to various charge densities if one bleached rhodopsin contributes one elementary charge. The interfacial translocation of one elementary charge per rhodopsin would correspond to an initial transmembrane potential of ~20 mV for a full bleach. This highly simplified picture also accounts rather well for the ionic strength dependence of the light-induced change, $\Delta A_f/A_f$, of spin label I in ROS membranes shown in Fig. 11. There are two features which make the light response of spin label I salt-dependent. First, the surface potential component of the boundary potential is salt-dependent. This effect decreases the magnitude of $\Delta A_f/A_f$ with increasing salt concentration. Second, as the salt concentration increases and the surface potential becomes less negative, the surface pH rises and the amount of protonated species decreases (Eq. 2). However, this latter effect is small at pH = 5.5, and[8]

[8]Since the relevant pK_a (Eq. 21) is 6.8 and the salt dependence is studied at pH = 5.5, the relatively small changes in surface pH with salt concentration will not produce significant changes in the fraction of the protein in the protonated

Eqs. 5–10 may be used to compute the expected salt dependence of $\Delta A_f/A_f$. The solid line in Fig. 11 is the result of the calculation taking one elementary charge translocated per photoactivated rhodopsin. The agreement between the experimental data and the calculated result may be viewed as further support for the model.

The reader should be reminded at this point that there is a reasonable degree of uncertainty in the calculated values of $\Delta A_f/A_f$ corresponding to any particular σ_{bo}^{ℓ}. The uncertainty arises largely because of our lack of information on the precise values of ϵ_b and ω as well as the drastic simplification of uniformly smeared charges. Nevertheless, the exercise is certainly worthwhile since it clearly demonstrates that the observed results can be readily explained on the basis of this simple electrostatic picture with reasonable choices of parameters.

Relation of the Photoresponse to the ERP

The early receptor potential (ERP) is a rapid photovoltage measured either by an intraretinal recording or by a recording of the corneal potential. The changes we have measured in the ROS membrane boundary potential (ψ_o^{ℓ}) correlate well with the known characteristics of the slow R_2 phase of the ERP: (*a*) Both the R_2 phase and the appearance of MII have a time-course very similar to that of the appearance of ψ_o^{ℓ} (Cone and Cobbs, 1969); (*b*) The ERP response and ψ_o^{ℓ} are both linear with the fraction of rhodopsin bleached (for $\psi_o^{\ell} \leq 25$ mV, $\Delta A_f/A_f$ is linear in ψ_o^{ℓ}); and (*c*) The ERP response from irradiation of MII has the opposite polarity of R_2, as does ψ_o^{ℓ} (Fig. 2, irradiation at 400 nm). In addition, the orientation of rhodopsin in the plasma membrane of the rod cell and the sign of the potential change of ψ_o^{ℓ} in the membrane are consistent with the positive outer-segment voltage measured for the R_2 phase of the ERP (Rüppel and Hagins, 1972). In fact, both Cone (1967) and Hong (1977) have suggested that the ERP might arise from an interfacial charge translocation rather than a charge separation within the membrane. Thus, it is suggested that the charge translocation which gives rise to a change in boundary potential measured by spin label (I) is very likely the source of the R_2 phase of the ERP.

Trissl et al. (1977) have reported observing a rapid photovoltage with rhodopsin incorporated into planar membranes. However, these photovoltages are pH-independent, are of shorter duration and much smaller magnitude than ψ_o^{ℓ}.

From the semiquantitative estimates of potential derived above, each rhodopsin molecule contributes ~20 nV to the instantaneous value of the transmembrane potential (and ψ_o^{ℓ}). This is on the order of the ERP signal per rhodopsin as estimated by Cone (1965), and is, as he argues, far too small for it to be involved directly as a transmission signal. On the other hand, if the potential changes observed here do indeed result from changes in charge density within a low dielectric region of the membrane, significant electrostatic coupling may result between rhodopsin molecules, particularly if they are clustered (Falk and Fatt, 1977).

As previously stated, an asymmetric change in the boundary potential on either side of a membrane will give rise to a change in transmembrane potential. In isolated ROS disk membranes, the change in ψ_o^{ℓ}, which gives rise to an instantaneous change in transmembrane potential upon bleaching, may prove to be a very useful tool. For example, when rhodopsin is bleached, the step change in $\Delta\psi$ which is produced decays with a time-course dependent upon

---

form. In fact for a surface charge density of -2.7×10^{-2} C/m^2 the fraction of bleached rhodopsin in the protonated form decreases by < 5% as the salt is increased from 0.001 to 0.5 M at pH = 5.5.

the conductance of the membrane. Thus, the decay rate provides a means of estimating relative membrane conductances to various ions immediately after bleaching. Such experiments are currently in progress.

We would like to thank Doctors Michael F. Brown, Stuart McLaughlin, James R. Trudell, and Juan Korenbrot for their comments and helpful discussions during the preparation of this manuscript. We also wish to thank Dr. Donald A. Glaser for allowing us unlimited use of his computer facility.

This research was supported by the National Institutes of Health grant EY 00729 and the Camille and Henry Dreyfus Foundation.

Received for publication 25 June 1979 and in revised form 9 November 1979.

REFERENCES

ABRAHAMSON, E. W. 1973. The kinetics of early intermediate processes in the photolysis of visual pigments. *In* Biochemistry and Physiology of Visual Pigments. H. Langer, editor. Springer-Verlag, Berlin. 47–56.

ANDERSEN, O., and M. FUCHS. 1975. Potential energy barriers to ion transport within lipid bilayers. *Biophys. J.* **15**:795–829.

ANDERSEN, O. S., S. FELDBERG, H. NAHADOMAN, S. LEVY, and S. MCLAUGHLIN. 1978. Electrostatic interactions among hydrophobic ions in lipid bilayer membranes. *Biophys. J.* **21**:35–70.

APPLEBURY, M. L., D. M. ZUCHERMAN, A. A. LAMOLA, and T. M. JOVIN. 1974. Rhodopsin. Purification and recombination with phospholipids assayed by the metarhodopsin I→metarhodopsin II transition. *Biochemistry.* **13**:3448–3458.

BENNETT, N. 1978. Evidence for differently protonated forms of metarhodopsin II as intermediates in the decay of membrane-bound cattle rhodopsin. *Biochem. Biophys. Res. Commun.* **83**:457–465.

CAFISO, D. S., and W. L. HUBBELL. 1978*a*. Estimation of transmembrane potentials from phase equilibria of hydrophobic paramagnetic ions. *Biochemistry.* **17**:187–195.

CAFISO, D. S., and W. L. HUBBELL. 1978*b*. Estimation of transmembrane pH gradients from phase equilibria of spin-labeled amines. *Biochemistry.* **17**:3871–3877.

CAFISO, D. S., and W. L. HUBBELL. 1979. Electrical and ion selective properties of rhodopsin containing membranes. *Biophys. J.* **25**:75*a*. (Abstr.)

CASTLE, J. D., and W. L. HUBBELL. 1976. Estimation of membrane surface potential and charge density from the phase equilibrium of a paramagnetic amphiphile. *Biochemistry.* **15**:4818–4831.

CHEN, Y. S., and W. L. HUBBELL. 1973. Temperature and light-dependent structural changes in rhodopsin-lipid membranes. *Exp. Eye Res.* **17**:517–532.

CONE, R. A. 1965. The early receptor potential of the vertebrate eye. *Cold Spring Harbor Symp. Quant. Biol.* **30**:483–491.

CONE, R. A. 1967. Early receptor potential: photoreversible charge displacement in rhodopsin. *Science (Wash. D.C.).* **155**:1128–1131.

CONE, R. A., and W. H. COBBS. 1969. Rhodopsin cycle in the living eye of the rat. *Nature (Lond.).* **221**:820–822.

EMRICH, H. M., and R. REICH. 1976. Effect of Ca^{2+} on the meta I-II transition. I. Experiments. *Pfluegers Arch Eur. J. Physiol.* **364**:17–21.

FALK, G., and P. FATT. 1977. Photosensitivity of electrical conductance of the rod disc membrane. *In* Vertebrate Photoreception. H. B. Barlow and P. Fatt, editors, Academic Press, Inc., New York. 77–95.

GRAFFNEY, B. J., and R. J. MICH. 1976. A new measurement of surface charge in model and biological lipid membranes. *J. Am. Chem. Soc.* **98**:3044–3045.

HOFFMANN, W., F. SIEBERT, K. HOFMANN, and W. KREUT. 1978. Two distinct rhodopsin molecules within the disc membrane of vertebrate rod outer segments. *Biochim. Biophys. Acta.* **503**:450–461.

HONG, F. T. 1977. Photoelectric and magneto-orientation effects in pigmented biological membranes. *J. Colloid Interface Sci.* **58**:471–497.

KETTERER, B., B. NEUMCKE, and P. LÄUGER. 1971. Transport mechanism of hydrophobic ions through lipid bilayer membranes. *J. Membr. Biol.* **5**:225–245.

KÜHN, H. 1978. Light-regulated binding of rhodopsin kinase and other proteins to cattle photoreceptor membranes. *Biochemistry.* **17**:4389–4395.

LEVINE, B. A., J. SACKETT, and R. P. J. WILLIAMS. 1979. Binding of organic ions to phospholipid bilayers. *Biochim. Biophys. Acta.* **550**:201–211.

LUNDSTRÖM, I. 1977. Influence of adsorbed charges and dipoles on the gating charges in excitable membranes. *FEBS (Fed. Eur. Biochem. Soc.) Lett.* **83**:7–10.

MATTHEWS, R. G., R. HUBBARD, P. K. BROWN, and G. WALD. 1963. Tautomeric forms of metarhodopsin. *J. Gen. Physiol.* **47**:215–240.

MELHORN, R. J., and L. PACKER. 1976. A spin label technique for monitoring the charge density of biomembranes. *Biophys. J.* **16**:194*a*. (Abstr.)

MCCONNELL, D. G., C. N. RAFFERTY, and R. A. DILLEY. 1968. The light-induced proton uptake in bovine retinal outer segment fragment. *J. Biol. Chem.* **243**:5820–5826.

MCLAUGHLIN, S. 1977. Electrostatic potentials at membrane-solution interfaces. *Curr. Top. Membranes Transp.* **9**:71–144.

NORISUYE, T., W. F. HOFFMAN, and H. YU. 1976. Intact photoreceptor membrane from bovine rod outer segment: size and shape in bleached state. *Biochemistry.* **15**:5678–5682.

PONTUS, M., and M. DELMELLE. 1975. Fluid lipid fraction in rod outer segment membrane. *Biochim. Biophys. Acta.* **401**:221–230.

PRATT, O., R. LIVINGSTON, and K. H. GRELLMAN. 1964. Flash photolysis of rod particle suspensions. *Photochem. Photobiol.* **3**:121–127.

RAPP, J. 1979. The kinetics of intermediate processes in the photolysis of bovine rhodopsin. II. The intermediate decay sequence from lumirhodopsin$_{492}$ to metarhodopsin$_{380}$II. *Vision Res.* **19**:137–141.

RÜPPEL, H., and W. A. HAGINS. 1973. Spatial origin of the fast photovoltage in retinal rod. *In* Biochemistry and Physiology of Visual Pigments. H. Langer, editor. Springer-Verlag, Berlin. 257–262.

SALE, G. J., P. TOWNER, and M. AKHTAR. 1977. Funtional rhodopsin complex consisting of three noncovalently linked fragments. *Biochemistry.* **16**:5641–5649.

SENGBUSCH, G. V., and H. STIEVE. 1971. Flash photolysis of rhodopsin. I. Measurements on bovine rod outer segments. *Z. Naturforsch.* **266**:488–564.

STEWART, J. G., B. N. BAKER, and T. P. WILLIAMS. 1977. Evidence for conformeric states in rhodopsin. *Biophys. Struct. Mech.* **3**:19–29.

TRISSL, H. W., A. DARSZON, and M. MONTAL. 1977. Rhodopsin in model membranes: charge displacements in interfacial layers. *Proc. Natl. Acad. Sci. U.S.A.* **74**:207–210.

TRISSL, H. W. 1979. Light-induced conformational changes in cattle rhodopsin as probed by measurements of the interface potential. *Photochem. Photobiol.* **29**:579–588.

TSIEN, R. Y. 1978. A virial expansion for discrete charges buried in a membrane. *Biophys. J.* **24**: 561–567.

VERMA, S. P., L. J. BERLINER, and I. C. P. SMITH. 1973. Cation-dependent light-induced structural changes in visual receptor membranes. *Biochem. Biophys. Res. Commun.* **55**:704–709.

WAGGONER, A. S., O. H. GRIFFITH, and C. R. CHRISTENSEN. 1967. Magnetic resonance of nitroxide probes in micelle-containing solutions. *Proc. Natl. Acad. Sci. U.S.A.* **57**:1198–1205.

WILLIAMS, T. P. 1975. Dynamics of opsin, a visual pigment. *Accounts Chem. Res.* **8**:107–112.